OXFORD

SOT | Society of Toxicology
www.toxsci.oxfordjournals.org

TOXICOLOGICAL SCIENCES, 157(2), 2017, 451–464

doi: 10.1093/toxsci/kfx062
Advance Access Publication Date: March 24, 2017
Research article

Mechanistic Insights in Cytotoxic and Cholestatic Potential of the Endothelial Receptor Antagonists Using HepaRG Cells

Matthew Gibson Burbank,[*,†,‡] Ahmad Sharanek,[*,†] Audrey Burban,[*,†] Hervé Mialanne,[‡] Hélène Aerts,[‡] Christiane Guguen-Guillouzo,[*,†] Richard John Weaver,[§,1] and André Guillouzo[*,†,1,2]

[*]Inserm UMR 991, Foie, Métabolismes et Cancer, Rennes, France; [†]Université Rennes 1, Rennes, France; [‡]Biologie Servier, Gidy 45520, France; and [§]Institut de Recherches Internationales Servier, Suresnes 92150, France

[1]These authors are senior co-authors.
[2]To whom correspondence should be addressed at Faculté de Pharmacie, INSERM UMR 991, Université de Rennes 1, F-35043 Rennes cedex, France. Fax: (33) 2 99 54 01 37. E-mail: andre.guillouzo@univ-rennes1.fr.

ABSTRACT

Several endothelin receptor antagonists (ERAs) have been developed for the treatment of pulmonary arterial hypertension (PAH). Some of them have been related to clinical cases of hepatocellular injury (sitaxentan [SIT]) and/or cholestasis (bosentan [BOS]). We aimed to determine if ambrisentan (AMB) and **mac**itentan (MAC), in addition to BOS and SIT, could potentially cause liver damage in man by use of human HepaRG cells. Our results showed that like BOS, MAC-induced cytotoxicity and cholestatic disorders characterized by bile canaliculi dilatation and impairment of myosin light chain kinase signaling. Macitentan also strongly inhibited taurocholic acid and carboxy-2',7'-dichlorofluorescein efflux while it had a much lower inhibitory effect on influx activity compared to BOS and SIT. Moreover, these three drugs caused decreased intracellular accumulation and parallel increased levels of total bile acids (BAs) in serum-free culture media. In addition, all drugs except AMB variably deregulated gene expression of BA transporters. In contrast, SIT was hepatotoxic without causing cholestatic damage, likely via the formation of reactive metabolites and AMB was not hepatotoxic. Together, our results show that some ERAs can be hepatotoxic and that the recently marketed MAC, structurally similar to BOS, can also cause cholestatic alterations in HepaRG cells. The absence of currently known or suspected cases of cholestasis in patients suffering from PAH treated with MAC is rationalized by the lower therapeutic doses and C_{max}, and longer receptor residence time compared to BOS.

Key words: endothelin receptor antagonists; cholestasis; hepatotoxicity; bile canaliculi; HepaRG cells.

Pulmonary arterial hypertension (PAH) is a rare, progressive disorder characterized by hypertension in pulmonary arteries with an estimated prevalence of 15–50 cases per million annually (Peacock *et al.*, 2007). The median survival for an untreated PAH patient with supportive care is 2.8 years after diagnosis and the overall prognosis remains guarded (D'Alonzo *et al.*, 1991; Velayati *et al.*, 2016). The pathogenesis of this disease is marked by enhanced synthesis of endothelin-1 (ET-1) and progressive proliferation and hypertrophy of smooth muscle cells in the pulmonary vasculature (Dupuis and Hoeper, 2008). Endothelin receptor antagonists (ERAs) are thought to offer appropriate treatment. They have the capacity to inhibit the binding of endothelin, a strong vasoconstrictive peptide, to its receptors on smooth muscle cells which results in a vasodilation in order

to decrease the pulmonary vascular pressure (Humbert *et al.*, 2004). Endothelin receptor antagonists have been shown to improve exercise tolerance and slow progression of disease in PAH patients (McLaughlin *et al.*, 2011). Two ERAs are currently approved in the United States under the name of bosentan (BOS) in 2001 and ambrisentan (AMB) in 2007. Another agent, sitaxentan (SIT), was approved in 2006 in Europe but not in the United States. Finally, a new ERA, macitentan (MAC), received approval in 2013. These ERAs have been differently associated with liver injury. In 2010, SIT was removed from the market due to concerns about its liver toxicity (Galiè *et al.*, 2011) and BOS was found to cause at least 3-fold upper limit of normal elevation of liver aminotransferases in about 16.8% of patients accompanied by elevated bilirubin in a small number of cases during clinical studies (Fattinger *et al.*, 2001). In contrast, AMB did not appear to cause hepatotoxicity with long-term treatment (Ben-Yehuda *et al.*, 2012). Although structurally similar to BOS, MAC has not been reported to cause elevation of liver transaminases or bilirubin. There is no data indicating that it has superior therapeutic potency to AMB (Sood, 2014). The 4 ERAs differ in their level of action on the 2 different ET-1 receptors, endothelin A receptor (ET_A) and endothelin B receptor (ET_B), which are G protein-coupled receptors whose activation results in elevation of intracellular free calcium (Davenport and Battistini, 2002). While MAC and BOS are dual antagonists, AMB and SIT are selective of ET_A (Dupuis and Hoeper, 2008). Ambrisentan is a propionic acid and the three others are sulfonamides. Bosentan, MAC, and SIT are direct inhibitors of the ATP binding cassette bile salt export pump (BSEP/ABCB11) as shown by using cells expressing human BSEP (Dawson *et al.*, 2012; Fattinger *et al.*, 2001; Lepist *et al.*, 2014). In contrast, MAC and its active metabolite ACT-132577 (Sidharta *et al.*, 2011) were reported to have no significant inhibitory effects on bile salt transport *in vivo* (Bolli *et al.*, 2012; Raja, 2010). *In vitro* studies suggest that hepatic disposition of MAC is mainly driven by passive diffusion rather than organic anion transporting polypeptide (OATP)-mediated uptake (Bruderer *et al.*, 2012). Mechanisms of ERAs hepatotoxicity remain poorly understood. Recently, we demonstrated that BOS and other cholestatic drugs cause alterations of bile canaliculi (BC) dynamics coupled with impairment of the RhoA/Rho-kinase/myosin light chain kinase (ROCK/MLCK) signaling pathway (Burbank *et al.*, 2016; Sharanek *et al.*, 2016). Interestingly, ERAs act by reducing myosin-actin interactions and myosin II contractile activity in smooth muscle and nonmuscle cells through phosphorylation of the myosin light chain by both ROCK and Ca^{2+}/calmodulin (CaM)-dependent MLCK (Dupuis and Hoeper, 2008; Miao *et al.*, 2002).

In the present work, we aimed to determine whether ERAs other than BOS are potentially cholestatic and to analyze the mechanisms involved in cytotoxic and cholestatic effects induced by the ERAs using human HepaRG cells. Our results showed that BOS and MAC shared in *in vitro* comparable cytotoxic and cholestatic properties while SIT was only cytotoxic and AMB was not hepatotoxic.

MATERIALS AND METHODS

Reagents. Macitentan and SIT were purchased from Alsachim (Illkirch-Graffenstaden, France). Bosentan (BOS) was obtained from Sequoia Research Products (Pangbourne, UK). Ambrisentan (AMB) was a gift from MSN Laboratories (Sanath Nagar, India). 1-Aminobenzotriazole (ABT) and methylthiazolete-tetrazolium (MTT) were purchased from Sigma (St. Quentin Fallavier, France). Calmodulin was from Merck Chemicals (Fontenay sous Bois, France). Phalloidin fluoprobe was obtained from Interchim (Montluçon, France). [^{3}H]-Taurocholic acid ([^{3}H]-TCA) was from Perkin Elmer (Boston, Massachusetts). Specific antibodies against phospho-myosin light chain 2 (ser19) (diluted 1:1000, catalog 3675) and HSC70 (Heat shock protein 70) were provided by Cell Signaling Technology (Schuttersveld, The Netherlands). Anti-zona occludens protein 1 (ZO-1) antibody was obtained from BD Biosciences (Le Pont de Claix, France). Anti-multidrug resistance-associated protein 2 (MRP2) and anti-multidrug resistance-associated protein 3 (MRP3) antibodies were from Abcam (Cambridge, UK) and secondary antibodies from Invitrogen (Saint Aubin, France). Hoechst dye was from Promega (Madison, Wisconsin). Other chemicals were of the highest reagent grade.

Cell cultures and treatments. HepaRG cells were seeded at a density of 2.6×10^4 cells/cm^2 in Williams' E medium supplemented with 2 mM glutaMAX, 100 U/ml penicillin, 100 μg/ml streptomycin, 10% Hyclone bovine fetal calf serum, 5 μg/ml insulin, and 50 μM hydrocortisone hemisuccinate. At confluence, after 2 weeks, HepaRG cells were transferred to the same medium supplemented with 1.7% dimethyl sulfoxide (DMSO) for 2 additional weeks in order to obtain confluent differentiated cultures containing nearly equal proportions of hepatocyte-like and progenitors/primitive biliary-like cells (Cerec *et al.*, 2007). These differentiated hepatic cell cultures were used for analytical assays. For drug treatments, differentiated HepaRG cells were incubated in a medium containing 2% serum and 1% DMSO. The list and characteristics of the 4 tested compounds are displayed in Table 1 and Supplementary Table 3.

Cell viability. Cytotoxicity of the test compounds was evaluated using the MTT colorimetric assay. Briefly, cells were seeded in 24-well plates and exposed to various concentrations of each compound in triplicate for 24 h. After medium removal, 100 μl of serum-free medium containing MTT (0.5 mg/ml) was added to each well and incubated for 2 h at 37 °C. The water-insoluble formazan was dissolved in 100 μl DMSO and absorbance was measured at 550 nm (Aninat *et al.*, 2006). IC20 values (the concentrations causing 20% cytotoxicity) were calculated from the concentration-responses curves.

Time-lapse cell imaging. Phase-contrast images of HepaRG cells were captured every 10 min, using time-lapse phase-contrast videomicroscopy. The inverted microscope Zeiss Axiovert 200M was equipped with a thermostatic chamber (37 °C and 5% CO_2) to maintain the cells under normal culture conditions and an Axiocam MRm camera with a 20× objective.

Determination of bile canalicular lumen surfaces. Bile canalicular lumen surfaces appeared bright (white) and the hepatocytes/biliary cells denser (black) using a phase-contrast microscope Zeiss Axiovert 200M. Brightness parameters were adjusted to eliminate noncorresponding objects and analysis was performed on at least 4 images per each condition (well). White canalicular lumen was then quantified using ImageJ software 1.48 every 10 min for 24 h. Data obtained during the first 4 h with all tested compounds are presented and BC quantification is expressed as percent of the control (Burbank *et al.*, 2016).

Myosin light chain kinase implication. Myosin light chain kinase implication was estimated using CaM, a specific MLCK activator (Sharanek *et al.*, 2016), at a 5 μM final concentration either alone (control) or in cotreatment with the dilatators (ie, BOS and

TABLE 1. Characteristics of the 4 ERAs

Compound	Affinity	C_{max}	Half-life ($t_{1/2}$) (h)	Dosing	Clinical Hepatic Effects	*In Vitro* Hepatic Effects	References
Ambrisentan	Selective for ET_A	2–3.2	15	5 or 10 mg once a day	No evidence of hepatotoxicity; better hepatic safety profile than for other ERAs	No modulation of MRP2, Pgp, or BSEP**	Barst (2007), Ben-Yehuda et al. (2012), and Takatsuki et al., 2013)
Bosentan	Dual antagonist ($50\times ET_A$)	6.75	5	62.5 mg then 125 mg two times a day	Elevated transaminases; increase in serum bile acids	BSEP and NTCP (Na^+-taurocholate cotransporting polypeptide) inhibition***; substrate for OATP. NTCP and MRP2**	Fattinger et al. (2001), Mano et al. (2007), Treiber et al. (2007), Dhillon and Keating (2009), and Hartman et al., 2010)Livertox website
Macitentan	Dual antagonist ($100\times E_A$)	0.13–0.75	16	10 mg once a day	Increased liver weight; centrilobular hypertrophy	BSEP and NTCP inhibition*; hepatic disposition mainly driven by passive diffusion	Ahn et al. (2014) and Lepist et al. (2014)Livertox website
Sitaxentan	Selective for ET_A ($6000\times ET_A$)	22	10	100 mg once a day	Elevated transaminases; dose-related increase in liver weight (centrilobular hypertrophy and necrosis)	NTCP and OATP transport Inhibition**; CYP3A4 inhibition	Dhaun et al. (2007), Hartman et al. (2010), Lavelle et al. (2009), Stavros et al. (2010), Galiè et al. (2011), Erve et al. (2013), and Chaumais et al. (2015)

The list of compounds, their affinity to the 2 endothelin receptors, C_{max} (μM), half-lives, dosing, clinical hepatic effects, and some results obtained *in vitro* with either vesicles overexpressing human BA transporters (*) or liver cells (**) are displayed. C_{max} values and *in vitro* results are from the literature (see references).

MAC). Bile canaliculi alteration was quantified after both drug treatment and drug/CaM cotreatment as described above.

Immunolabeling. Cells were washed with warm phosphate buffered saline (PBS), fixed with 4% paraformaldehyde for 20 min at room temperature, and then washed three times with cold PBS. After paraformaldehyde fixation, cells were permeabilized for 20 min with 0.3% Triton in PBS followed by 1-h incubation in PBS containing 1% bovine serum albumin and 5% normal donkey serum. Cells were then incubated overnight with primary antibodies directed against ZO-1, MRP2 (MRP2/ABCC2) and MRP3 (MRP3/ABCC3), and washed with cold PBS before 2-h incubation with mouse or rabbit Alexa fluor 488 labeled secondary antibodies in the same buffer as described above. Cells were washed with cold PBS and incubated with rhodamine-phalloidin fluoprobe SR101 (200 U/ml) diluted at 1/100 for F-actin labeling for 20 min (Pernelle *et al.*, 2011). After washing with cold PBS, cells were incubated with Hoechst in PBS for 20 min for nuclei labeling. Immunofluorescence images were detected by Cellomics ArrayScan VTI HCS Reader (Thermo Fisher Scientific, Waltham, Massachusetts) (Bachour-El Azzi *et al.*, 2015).

CDF excretion. After 2 h of exposure to the drugs in serum-free medium, cells were incubated for 20 min at 37 °C with 3 μM 5-(and 6)-carboxy-2',7'-dichlorofluorescein diacetate (CDFDA), which is hydrolyzed by intracellular esterases to CDF (5- (and 6)-carboxy-2',7'dichlorofluorescein), a substrate of MRP2. After washing, imaging was done using inverted microscope Zeiss Axiovert 200M and AxioCam MRm (Sharanek *et al.*, 2014).

Taurocholic acid clearance. To evaluate taurocholic acid (TCA) clearance activity, cells were first exposed to 43.3 nM [^{3}H]-TCA for 30 min to induce its intracellular accumulation, then washed with standard buffer and incubated with the test compounds for 2 h in a standard buffer with Ca^{2+} and Mg^{2+}. After incubation with test compounds, cells were washed and scraped in 0.5 N NaOH and the remaining radiolabeled substrate was measured through scintillation counting to determine [^{3}H]-TCA clearance (Anthérieu *et al.*, 2013). Taurocholic acid influx was estimated by determination of sodium-dependent intracellular accumulation of the radiolabeled [^{3}H]-TCA substrate. Cells were treated with the 4 drugs for 2 or 24 h followed by incubation with radiolabeled TCA for 30 min. Cells were then washed with PBS and lysed with 0.1 N NaOH. Accumulation of radiolabeled substrate was determined through scintillation counting (Anthérieu *et al.*, 2013). [^{3}H]-TCA clearance was determined based on its accumulation in the cell layers (cells + BC) and calculated relative to the control using the following formula: [^{3}H]-TCA clearance = ([^{3}H]-TCA accumulation in $(\text{cells} + \text{BC})_{\text{Control}} \times 100$)/([^{3}H]-TCA accumulation in cell layers)$_{\text{Tested compound}}$ (Sharanek *et al.*, 2016).

Real-time quantitative polymerase chain reaction analysis. Total RNA was extracted from 10^6 HepaRG cells with the SV total RNA isolation system (Promega, Charbonnieres-les-Bains, France). RNAs were reverse- transcribed into cDNA and real-time quantitative polymerase chain reaction (RT-qPCR) was performed using a SYBR Green mix. Primer pair sequences are listed here: *GAPDH* (ID 2597), forward, 5′-ttcaccaccatggagaaggc-3′: reverse, 5′-ggcatggactgtggtcatga-3′; *BSEP* (ID 8647), forward, 5′-tgatcctgatcaagggaagg-3′: reverse, 5′-tggttcctgggaaacaattc-3′; *NTCP* (ID 6554), forward, 5′-gggacatgaacctcagatt-3′: reverse, 5′-cgttggatttgaggacgat-3′; *OATP-B* (ID 6579), forward, 5′-tgattggtatggggctatc-3′: reverse, 5′- catatcctagggctggtgt-3′; *MRP2* (ID 1244), forward, 5′-tgagcaagtttgaaacgcacat-3′: reverse,

5′-agctcttctcctgccgtctct-3′; *MRP3* (ID 8714), forward, 5′-gtccgcagaatggacttgat-3′: reverse, 5′-tcaccacttggggatcatt-3′; *MRP4* (ID 10257), forward, 5′-gctcaggttgcctatgtgct-3′: reverse, 5′-cggttacaatttcctcctcca-3′.

Western blotting analysis of p-myosin light chain subunit-2. HepaRG cells were treated with the tested compounds for 1, 2, and 3 h at 100 μM where BC alteration occurred, then washed with cold PBS and finally resuspended in cell lysis buffer supplemented with protease and phosphatase inhibitors (Roche, Mannheim, Germany). Aliquots containing equivalent total protein content, as determined by the Bradford procedure with bovine serum albumin as the standard, were subjected to sodium dodecyl sulfate/12% polyacrylamide gel electrophoresis, electrotransferred to immobilon-p membranes, and incubated overnight with primary antibodies directed against p-myosin light chain subunit-2 (MLC2) and HSC70. After using a horseradish peroxidase conjugated anti-mouse/rabbit antibody (Thermo-Fisher Scientific, Waltham, Massachusetts), membranes were incubated with a chemiluminescence reagent (Millipore, Billerica, Massachusetts) and bands were visualized and quantified by densitometry with fusion-CAPT software (Vilber Lourmat, Collégien, France).

Measurement of endogenous bile acid content. In order to avoid any bile acid (BA) contamination from the serum, all treatments and washings were done in serum-free media. Both dried cell pellets and 1 ml medium samples were collected for BA analysis from HepaRG cell cultures exposed to different drug concentrations at various time points. The BA content was measured using ultra high-pressure liquid chromatography coupled with tandem mass spectrometry (UPLC–MS/MS). An Acquity UPLC BEH Waters column (Waters Corporation, Milford, Massachusetts), thermostated at 65 °C, was used for chromatographic separation of BA. Mobile phases consisted of (A) (0.1% HCOOH in purified water) and (B) (0.05% triethylamine in acetonitrile) at 95:5 (v/v). Bile acids were eluted by increasing B/A ratio from 5 to 95 (v/v) for 14.5 min. Separation was achieved at a flow rate of 0.35 ml/min for 18 min. Mass spectra were obtained using an API4000 SCIEX (AB-Sciex, Framingham, Massachusetts). Data were acquired by Software Analyst (ABSCIEX) V 1.6.1; Software Masslynx (Waters) V 4.1 and Software Watson (Thermo-Fisher scientific) V 7.3.0.01. The amount of individual BAs in each medium sample was calculated as pmol/ml (nM) and in cell lysate samples as pmol and scaled per mg of proteins. Because basal primitive biliary cells do not express BAs metabolizing enzymes as well as BA transporters (Sharanek *et al.*, 2015) they were neglected for calculation of BA synthesis. Only HepaRG hepatocytes were considered and estimated to represent 50% of total cells in HepaRG cell cultures (Cerec *et al.*, 2007). Total cholic acid (CA) represented the sum of (unconjugated CA + TCA + GCA) whereas total chenodeoxycholic acid (CDCA) represented the sum of (unconjugated CDCA + TCDCA + GCDCA).

Statistical analysis. One-way ANOVA with multiple comparison test (graphpad prism 6.00) was performed to compare time-dependent MLC2 phosphorylation in different samples. Data were considered significantly different when $^{*}P < .05$. One-way ANOVA with Bonferroni's multiple comparison test (GraphPad Prism 6.00) was performed to compare BAs data. Each value corresponded to the mean ± standard error of mean (SEM) of at least three independent experiments. Data were considered significantly different when $^{*}P < .05$. The Student *t*-test was also applied to compare values of cytotoxicity, TCA clearance and mRNA levels between treated and corresponding control cultures. Data were considered as significantly different when $^{*}P < .05$. For the mRNA levels, data were also considered as significantly different with the 4 h treatment when $^{\#}P < .05$. Each value corresponded to the mean ± SEM of three independent experiments.

RESULTS

Cytotoxic Potential of ERAs

Preliminary experiments were performed to calculate IC20 values for the 4 drugs after a 24-h treatment of HepaRG cells with a range of drug concentrations from 0 to 800 μM using the MTT assay (Figure 1A). The most cytotoxic compound was BOS with an IC20 value of 120 μM followed by MAC (230 μM) and SIT (580 μM). Ambrisentan was not cytotoxic in the range of concentrations tested. In order to determine whether cytotoxicity was related to cytochrome P450 (CYP)-mediated formation of toxic metabolites a set of cultures was cotreated with ERAs and 300 μM 1-ABT, a nonselective inhibitor of human P450s, for 24 h. Cotreatment with ABT markedly reduced SIT and BOS cytotoxicity at high concentrations (ie, at 400 and 800 μM, respectively) (Figure 1B) while it did not alter effects of MAC.

Bosentan and Macitentan Caused Morphological Alterations of Bile Canaliculi

We have previously shown that cholestatic drugs cause constriction or dilatation of BC after a short treatment of HepaRG cells (Burbank *et al.*, 2016; Sharanek *et al.*, 2016). In the present study, we analyzed effects of ERAs on BC dynamics over a 4-h period using time-lapse videomicroscopy imaging.

Macitentan and BOS induced dilatation of BC, starting within the first hour whereas SIT and AMB did not affect BC dynamics (Figure 2A) (Supplementary videos). Interestingly, even at 400 μM, corresponding to a cytotoxic concentration for both BOS and MAC, the two other ERAs, SIT, and AMB, did not affect BC dynamics (Figure 2D) (Supplementary videos). At 600 μM (ie, around IC20 value), SIT caused some morphological alterations without any change in BC structures (Figure 2D). Bile canaliculi alterations caused by BOS and MAC were quantified by measuring the canalicular surface using the ImageJ software every 10 min for 180 min BC dilatation was greater with MAC than with BOS (Figure 2B). Immunolocalization of the junctional zona occludens protein 1 (ZO-1) and pericanalicular F-actin did not evidence any obvious disruption of BC integrity associated with dilatation of the canalicular lumen at 2 h or longer treatments (Figure 2C).

Myosin Light Chain Subunit-2 and MLCK Impairment

It has been postulated that dynamic movements of BC could be controlled by pericanalicular myosin activity (Sharanek *et al.*, 2016). Treatment with BOS and MAC, the two drugs that induced BC dilatation, showed a decrease with time in MLC2 phosphorylation while AMB and SIT were ineffective (Figures 3A and B). Because MLCK is coupled to ROCK and shares MLC2 as a common substrate, we evaluated whether MLCK also contributed to BC lumen alterations. Myosin light chain kinase implication in BC deformations was determined by the use of CaM, a specific MLCK activator. HepaRG cells were treated with CaM in the presence of dilatators (Burbank *et al.*, 2016; Sharanek *et al.*, 2016) and BC alterations were quantified and compared to treatment with the modulator alone as described above. Cotreatment with 5 μM CaM partly counteracted dilatation

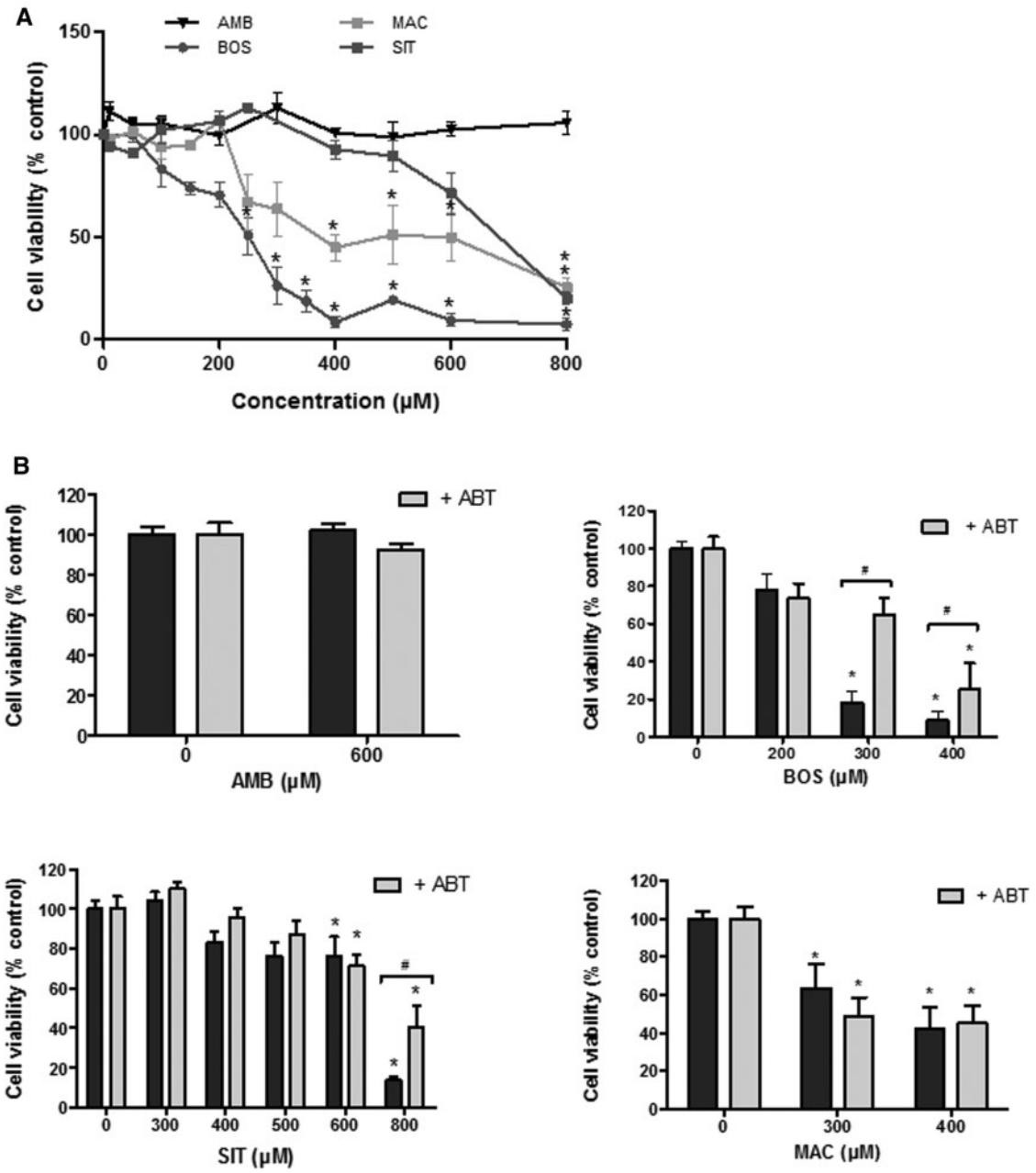

FIG. 1. Cytotoxicity of the 4 ERAs. HepaRG cells were treated with different concentrations of the 4 ERAs in the absence (A) or presence (B) of ABT (300 μM) for 24 h. Cytotoxicity was measured by the MTT colorimetric assay. Each point is the mean ± SEM of three independent experiments. Data were considered as significantly different from the cells treated only with ABT when $^{\#}P < .05$. Data were considered as significantly different from the control when $^{*}P < .05$.

induced by BOS and MAC while treatment with CaM 5 μM alone did not cause any effect on BC (Figures 3C and D).

Bile Acid Profile Changes

Bile acid profiles were analyzed after treatment of HepaRG cells with 10, 50, and 100 μM of each drug for 4 or 24 h in serum-free medium. Interestingly, a dose-dependent intracellular decrease and parallel accumulation in supernatants of total BAs were observed with MAC, BOS, and SIT at both time points (Figure 4). Ambrisentan did not cause any effect. At 100 μM MAC showed a decrease in BA intracellular accumulation dropping from 15.7 (control value) to 5 and 2 pmol/mg proteins, respectively, while BA content increased in the supernatant from 25 to 64 nM and 34 to 78 nM after 4 and 24 h treatment, respectively (Figure 4C). Bosentan exhibited approximately the same pattern, ie, a decrease from 22 to 6 pmol/mg proteins in cellular layers and from 24 to 3 pmol/mg proteins after 4 and 24 h, respectively; in supernatants, values varied between 31 and 46 nM at 4 h and 51 and 67 nM at 24 h (Figure 4B). At 100 μM SIT showed a more important decrease in total BAs in cellular layers ranging from 15 to 4 pmol/mg proteins and 15 to 2 pmol/mg proteins after 4 and 24 h, respectively. Concomitantly, BAs concentrations in the supernatant increased from 39 to 69 nM and 54 to 78 nM at 4 and 24 h of treatment with this drug (Figure 4D). Finally, AMB had no effect on BAs intracellular accumulation (around 19 pmol/mg proteins) and supernatant levels (between 33 and 70 nM) at all tested concentrations and at the two treatment time points (Figure 4A). Changes were also estimated as

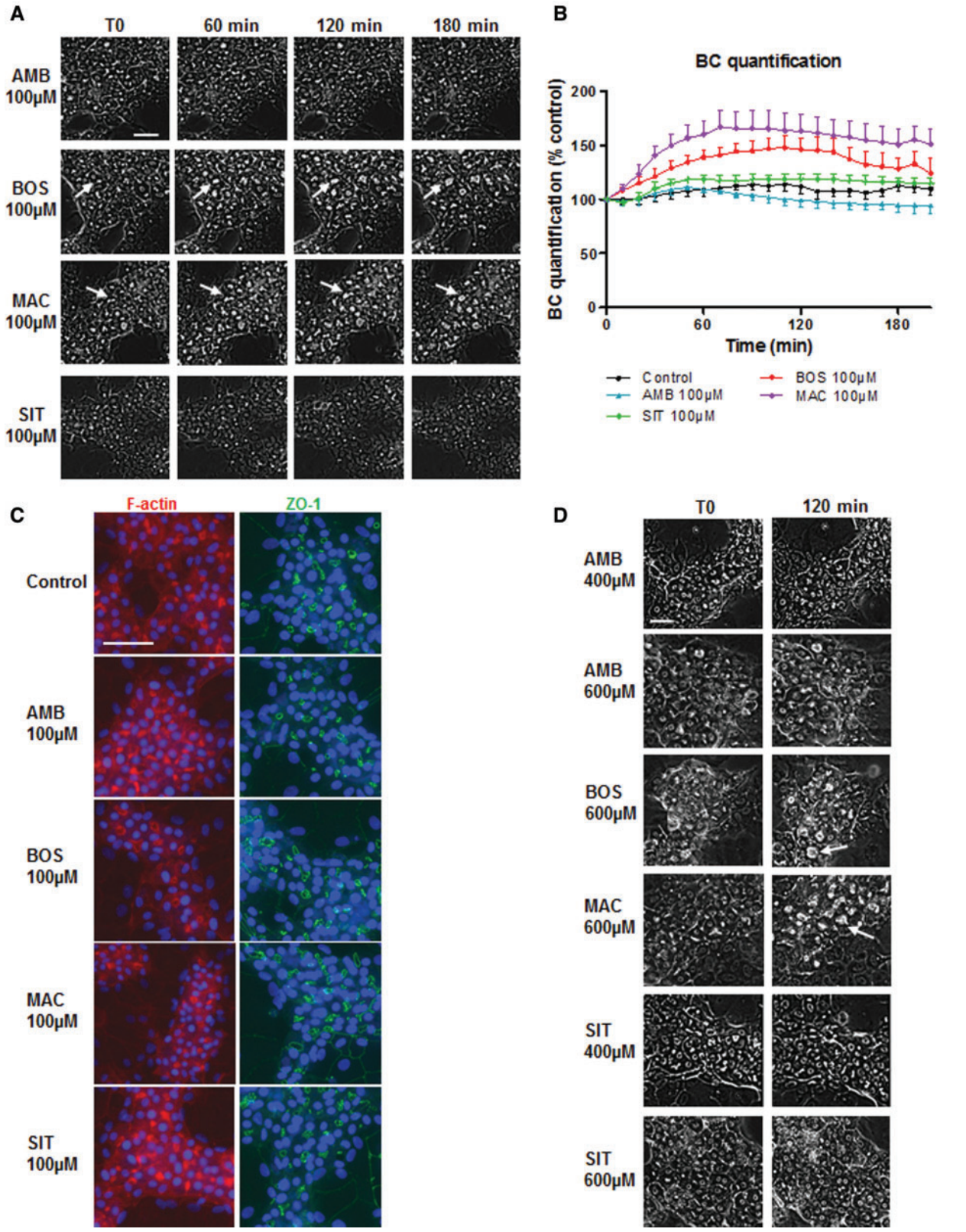

FIG. 2. Effects of drugs on bile canaliculi dynamics. (A) Phase-contrast micrographs of HepaRG cells exposed to 100 µM of each drug at 3 different time-points. Arrows show BC dilatation. (B) BC surfaces of control and treated cells quantified on the basis of brightness parameters. White canalicular lumen was quantified using image-J software every 10 min. Data were expressed relative to untreated cells, arbitrarily set at 100%. Data represent the means ± SEM of three independent experiments. Dilatators at least transiently enlarged BC >125%. (C) F-actin localization using rhodamine-phalloidin fluoroprobe (red). Junctional ZO-1 immunolabeling (green) in control and treated cells. Nuclei stained using the Hoechst dye. Fluorescence appears white in black and white micrographs. (D) Phase-contrast micrographs of HepaRG cells at 0 and 120 min. Cells were exposed to different drug concentrations. Arrows show BC dilatation. Bar = 30 µM.

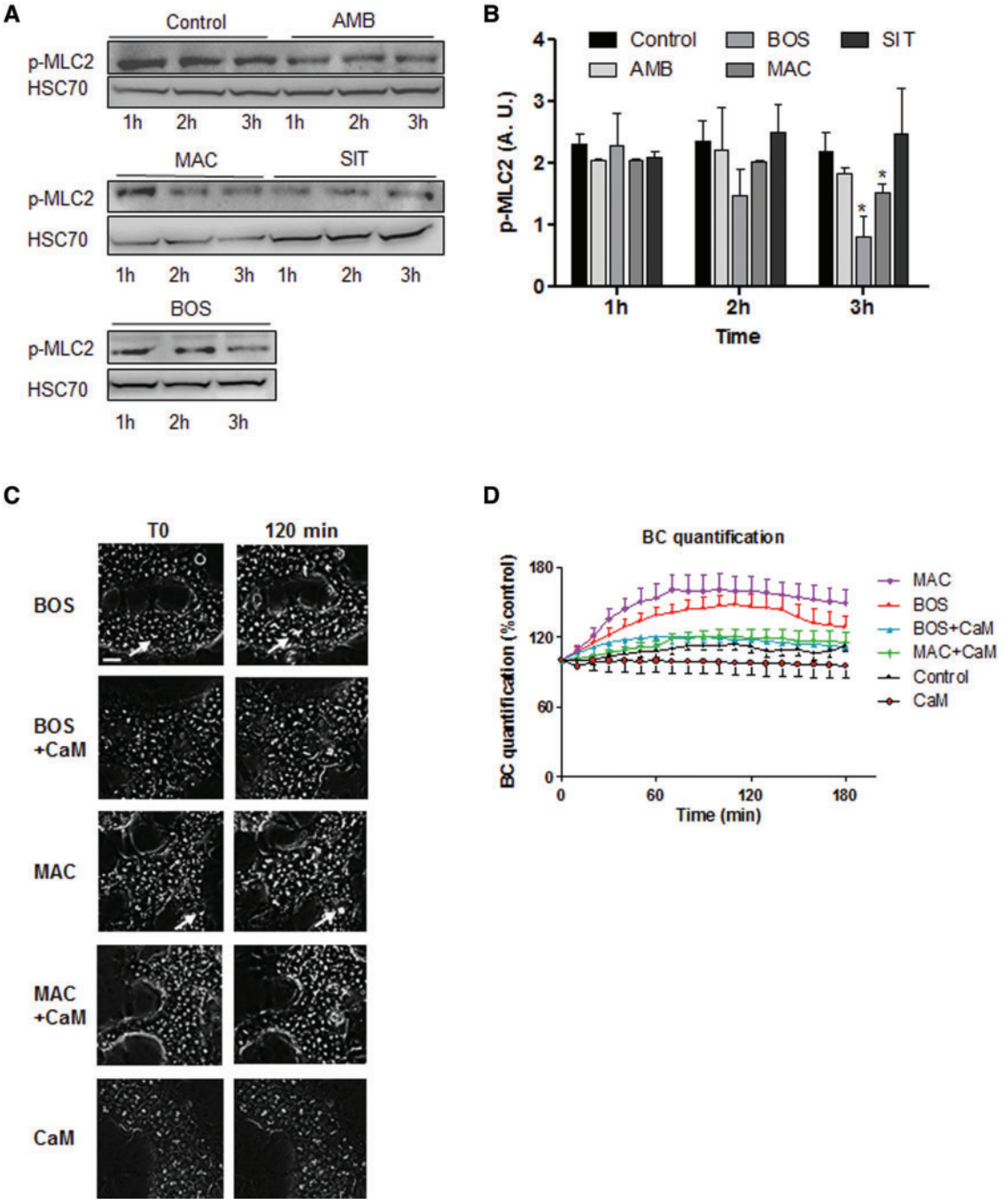

FIG. 3. Effects of drugs on MLC2 phosphorylation state and BC morphology. (A) Representative Western blots of p-MLC2 compared to HSC70 at 1, 2, and 3 h in ERA-treated cells. (B) Graphical representation of MLC2 phosphorylation/dephosphorylation quantification using fusion-CAPT software. Data are expressed in arbitrary units (A.U.) and represent means ± SEM of 3 independent experiments. One hour treatment was arbitrarily set at a fixed value of 2.5 for all drugs. Data were considered significantly different when *$P < .05$. (C, D) Cells treated with 100 μM BOS or MAC ± 5 μM CaM for 2 h. Phase-contrast images and BC surface quantification as described in Figure 2B. Arrows show BC dilatation. Bar = 30 μM.

percentages in comparison with controls and individual BAs were measured. As shown in Supplementary Tables 1 and 2, all individual BAs have the same tendency to decrease in cellular layers and to increase in supernatants.

Effects on Taurocholic Acid Influx and Canalicular Efflux Activities

To confirm whether ERA-induced BC deformations were associated with alterations of BA transport, influx and efflux activities were measured using [^{3}H]-TCA as a substrate. As shown in Figures 4E, G, and H, AMB had no significant effect on either influx or efflux activities. Macitentan and BOS inhibited TCA efflux, starting at 10 (13–76× C_{max}) and 50 μM (7× C_{max}) for MAC and BOS, respectively, whereas SIT activated efflux activity at low concentration (10 μM) and was ineffective at 50 μM and higher concentrations (Figure 4E). These concentrations represent 0.5× and 2× C_{max}. To confirm its greater activity at 10 μM, SIT was also tested at 1, 5, and 20 μM. Intermediate increased values were obtained confirming the concentration-dependent

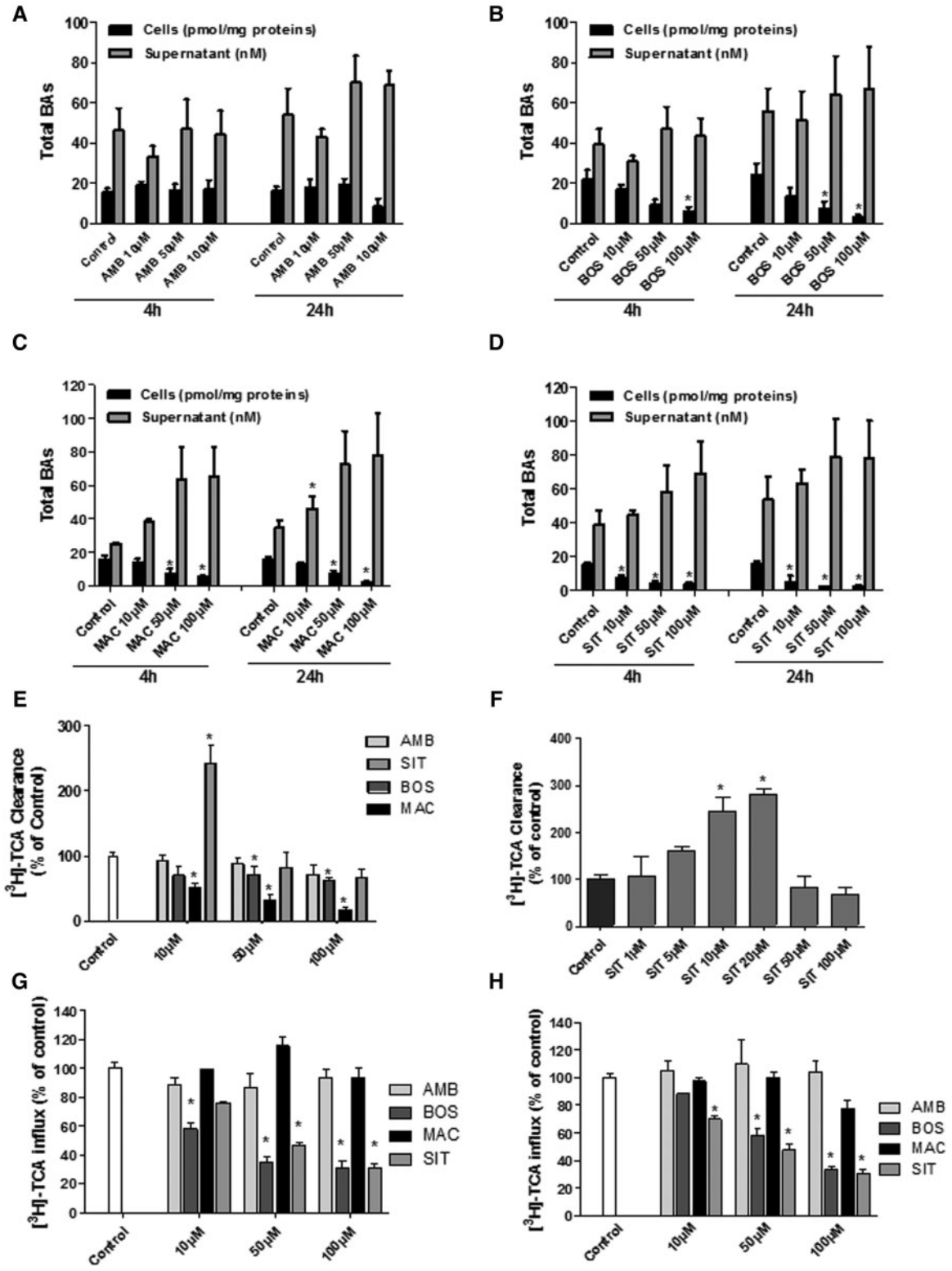

FIG. 4. Drug effects on total BA disposition and TCA influx and clearance. (A-D) BAs measured in supernatants (nM) and cell layers (pmol/mg proteins) after treatment with different drug concentrations for 4 and 24 h and in corresponding controls. Data were normalized relative to the amount of proteins. (E) [^{3}H]-TCA clearance in cells treated with different drug concentrations after 2 h. (F) [^{3}H]-TCA clearance with additional SIT concentrations after 2 h. (G, H) [^{3}H]-TCA influx in treated cells at 2 and 24 h. Values represent the sum of mean ± SEM of duplicate measurements in 3 independent experiments; *$P < .05$ compared to values in corresponding controls.

induction of TCA efflux by SIT, peaking at around 20 μM (Figure 4F). Taurocholic acid influx was inhibited by BOS and SIT; activity started to decrease with both drugs at 10 μM after 2 h treatment (Figure 4G). After 24 h SIT and BOS still exerted an inhibitory effect starting at 10 and 50 μM, respectively. Macitentan and AMB did not influence TCA influx (Figure 4H).

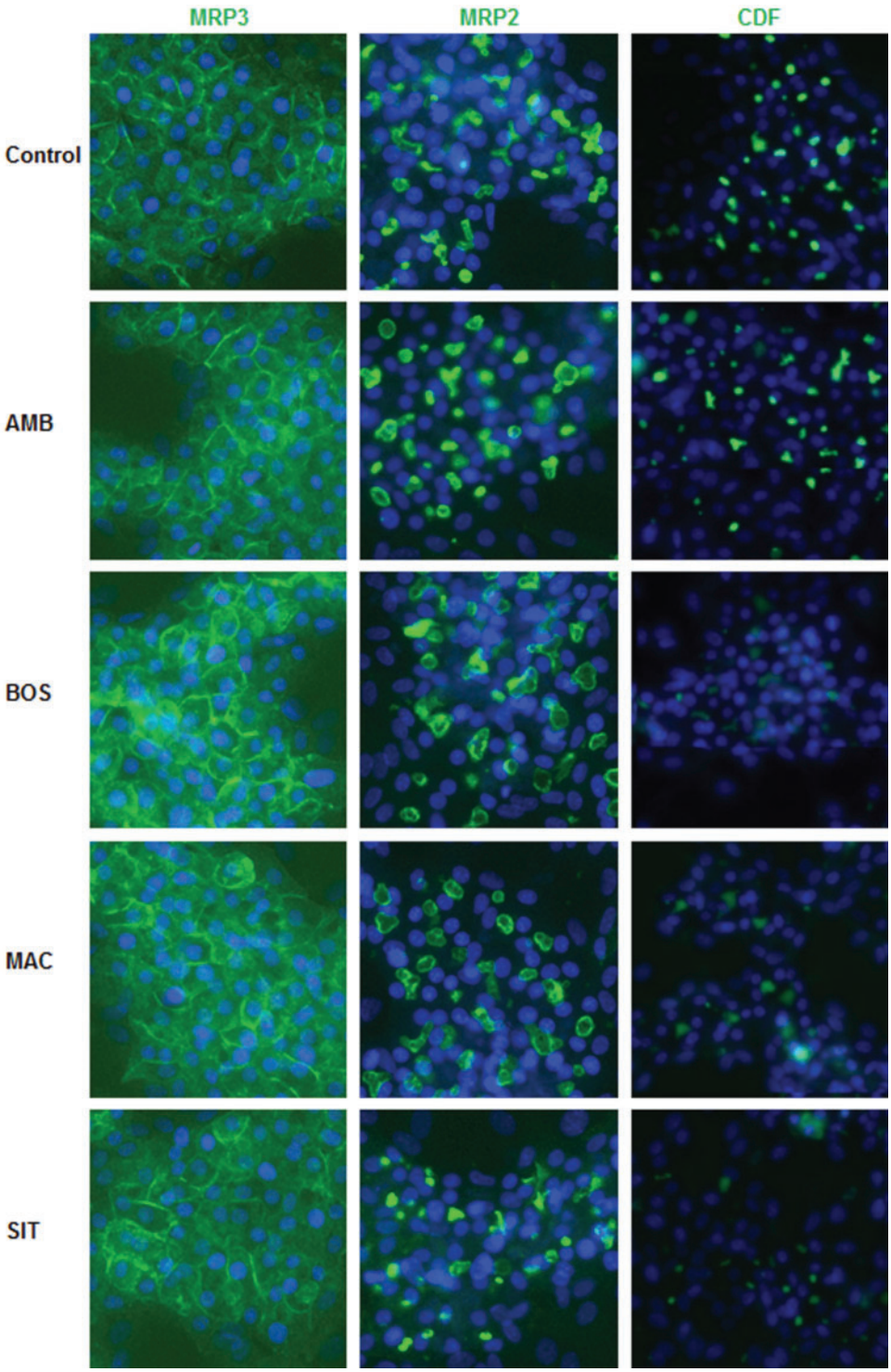

FIG. 5. MRP3 and MRP2 distribution and MRP2 functional activity. Differentiated HepaRG cells were fixed after 2 h treatment and incubated with primary antibodies against MRP3 and MRP2 (green fluorescence). MRP2 activity was estimated using CDFDA. Efflux of fluorescent CDF, a substrate of MRP2, characterized by accumulation of green fluorescence into bile canaliculi, was evaluated in standard buffer. Nuclei stained using the Hoechst dye. Immunofluorescence images were obtained with a Cellomics ArrayScan VTI HCS Reader. Fluorescence appears white in black and white micrographs. Bar = 30 μM.

Multidrug Resistance-Associated Protein 3 and MRP 2 Immunolabeling Intensity

After 2 h treatment, distribution of MRP3 protein was analyzed using immunolabeling (Figure 5). Compared to untreated cells, immunostaining intensity of MRP3 to the basolateral membrane of HepaRG cells was slightly increased with the 4 ERAs. Distribution of MRP2 was also analyzed after 2 h treatment with the 4 drugs using a specific antibody. Compared to untreated cells, immunostaining of MRP2 to the apical membrane of HepaRG cells was slightly decreased with BOS, MAC, and SIT.

TABLE 2. Effects of the 4 Drugs on Transcript Levels of the Basolateral Transporters

Drugs (μM)		Bile Acids Transporters					
		BSEP (ABCB1)	*NTCP (SLC10A1)*	*OATP-B (SLC21A9)*	*MRP2 (ABCC2)*	*MRP3 (ABCC3)*	*MRP4 (ABCC4)*
AMB	**10**	0.88±0.08	0.87±0.07	1.03±0.13	1.00±0.12	0.99±0.09	1.04±0.06
	50	0.94±0.09	0.89±0.09	1.01±0.09	1.12±0.07	1.06±0.11	1.09±0.07
	100	1.00±0.1	0.99±0.11	0.97±0.02	1.14±0.15	1.08±0.16	1.14±0.07
BOS	**10**	0.59±0.04*	0.82±0.09	0.95±0.12	1.35±0.23	0.84±0.08	1.16±0.12
	50	0.23±0.04*	0.45±0.10*	0.50±0.10*	1.17±0.03	0.60±0.08*	1.01±0.11
	100	0.11±0.01*	0.23±0.06*	0.41±0.07*	0.99±0.16	0.62±0.09*	1.08±0.16
MAC	**10**	0.73±0.05	0.72±0.06	1.07±0.12	1.49±0.18*	1.00±0.07	1.04±0.08
	50	0.69±0.18	0.50±0.06*	0.99±0.07	1.46±0.15*	0.98±0.08	1.13±0.09
	100	0.40±0.7*	0.22±0.05*	0.78±0.12	1.78±0.19*	0.89±0.23	1.34±0.06
SIT	**10**	0.97±0.16	0.78±0.06	0.98±0.04	1.23±0.04	0.92±0.01	1.05±0.01
	50	0.88±0.10	0.50±0.04*	0.95±0.09	1.37±0.18	1.02±0.17	1.07±0.05
	100	0.91±0.22	0.23±0.05*	0.90±0.27	1.53±0.23	1.04±0.18	1.22±0.10

HepaRG cells were exposed to the 4 drugs at the indicated concentration (ie, 10, 50, or 100 μM) for 24 h. mRNA levels were measured by RT-PCR analysis. All results are expressed relative to the levels found in control cells, arbitrarily set at a value of 1.
*$P < .05$ compared to untreated cells.

Carboxy-2',7'-dichlorofluorescein Canalicular Accumulation

Fluorescent CDF, predominantly excreted by MRP2, was also visualized in BC of untreated and treated HepaRG cells. While AMB did not show any significant effect compared to control cells, SIT, MAC, and BOS exerted an inhibition of CDF accumulation in the BC (Figure 5).

Modulation of Bile Acid Transporters Gene Expression

Genes encoding the major BA transporters are also deregulated by cholestatic drugs (Pauli-Magnus and Meier, 2006). Six major genes encoding either efflux (*BSEP*, *MRP2*, *MRP3*, *MRP4*) or uptake (*NTCP*, *OATP-B*) transporters were analyzed by RT-qPCR after 4, 8, or 24 h treatment with 3 concentrations of each tested drug (ie, 10, 50, and 100 μM). Different patterns depending on the compound and the tested concentration were evidenced and are shown in Table 2 and Supplementary Figures 1–3. Ambrisentan did not deregulate any of the transporters at the 3 concentrations used whatever the duration of treatment (4, 8, and 24 h). In contrast, variable effects were observed with the 3 other drugs. *Bile salt export pump (BSEP)* was strongly repressed by BOS starting at 8 h and by MAC only at high concentrations after 24 h (Table 2; Supplementary Fig. 2). *Na^+-taurocholate cotransporting polypeptide (NTCP)* was downregulated starting at 24 h for the two high concentrations (ie, 50 and 100 μM) of BOS, MAC, and SIT. *Multidrug resistance-associated protein 2 (MRP2)* was upregulated with MAC and SIT at the two highest concentrations (Table 2; Supplementary Fig. 1). *Organic anion transporting polypeptide-B* (*OATP-B*) and *MRP3* were decreased only with BOS starting after 8 h at the highest concentrations (Table 2; Supplementary Figures 2 and 3) and *MRP4* was not modulated by any of the drugs (Table 2; Supplementary Fig. 3).

DISCUSSION

In the current work, we showed MAC shares similar cholestatic features with BOS while SIT exhibited only cytotoxic effects. In contrast, AMB showed no features of hepatotoxicity across the broad range of concentrations tested.

Cytotoxicity of SIT and BOS observed in *in vitro* are supported by reports on hepatocellular injury in treated patients (Fattinger *et al.*, 2001; Galiè *et al.*, 2011; Lavelle *et al.*, 2009). Sitaxentan was found to induce hypertrophy and necrosis of centrilobular hepatocytes in dogs (Lin *et al.*, 2012), and to cause severe liver injury with 8 deaths during clinical trials (Owen *et al.*, 2012). Even though SIT was reported to inhibit BSEP activity in BSEP-expressing membrane vesicles (Morgan et al., 2013), no clinical reports had shown its cholestatic potential. These false positive results could be related to the lack of metabolism in the vesicles. Indeed, SIT undergoes several enzymatic reactions with the involvement of various CYPs, including CYP2C9 and CYP3A4, that lead to a reactive ortho-quinone metabolite which is able to form adducts with glutathione (Erve *et al.*, 2013). Our data agree with the implication of reactive metabolites in the induction of hepatocellular injury. Indeed when CYP activities were inhibited by addition of the nonspecific CYP inhibitor ABT, toxicity was reduced. Importantly, SIT was approved for use in clinical trials at a daily dose of 100 mg and 300 mg/day and idiosyncratic hepatotoxicity is known to occur more frequently with drugs administered at >50 mg/day (de Abajo *et al.*, 2004).

In the 5-year EARLY study, 16.8% PAH patients treated with BOS showed elevation of transaminases superior to 3-fold the upper limit of normal, mostly within the first 6 months of treatment (Simonneau *et al.*, 2014). Bosentan was found to cause toxicity in primary human hepatocytes; it is a strong PXR activator (Weiss *et al.*, 2013) and is mainly metabolized by CYP3A4 and CYP2C9 (Gatfield *et al.*, 2012) into 4 metabolites. As expected, cotreatment with ABT also reduced its toxicity (Matsunaga *et al.*, 2016). Our data with HepaRG cells treated with ABT fully agrees with this study concluding that at least one BOS CYP-mediated metabolite is potentially hepatotoxic. Noticeably, because combined treatment with phosphodiesterase 5 inhibitors and other drugs is used for the treatment of PAH (Ghofrani *et al.*, 2011) different interactions between BOS and other drugs could be expected to contribute to greater liver damage.

Contrary to BOS and SIT, AMB and MAC are not known to induce hepatocellular injury in man. In agreement with clinical data (Barst, 2007; Takatsuki *et al.*, 2013), AMB was not toxic to HepaRG cells. It is mainly metabolized by UGTs; only 20% undergoes oxidative metabolism via CYP3A4 and to a lesser extent CYP3A5 and CYP2C19 (Croxtall and Keam, 2008). Noteworthy, AMB is used at 5 mg/day, a low concentration compared to other ERAs (Chaumais *et al.*, 2015; Takatsuki *et al.*, 2013). Macitentan was cytotoxic to HepaRG cells but at higher concentrations than BOS (IC20 values: 230 vs 120 μM, respectively). Moreover, MAC toxicity was not reduced by a

TABLE 3. Summary of the Results on the 4 ERAs

Compound	IC20	BC deformation	[^{3}H]-TCA clearance (ctrl=100%)	BSEP mRNA expression (ctrl=1)	MLC2 phosphorylation state	MLCK implication
Ambrisentan 100 μM	>800	nc	73.2±15.4	1.0±0.0	nc	–
Bosentan 100 μM	120	Dilatation	64.24±3.2*	0.4±0.2*	Dephosphorylation	MLCK
Macitentan 100 μM	230	Dilatation	19.4±2.9*	0.77±0.2*	Dephosphorylation	MLCK
Sitaxentan 100 μM	580	nc	68.7±13.7	1.03±0.1	nc	–

IC20 (μM), BC deformation (ie, constriction or dilatation), [^{3}H]-TCA clearance (control = 100%), *BSEP* mRNA expression (control = 1), MLC2 phosphorylation state and MLCK implication are summarized.
Abbreviations: BC, bile canaliculi; ROCK, Rho-kinase; MLCK, myosin light chain kinase; nc, no change.

cotreatment with ABT, supporting that its toxicity was not CYP-mediated. In agreement, although MAC is mainly metabolized by CYP3A4 and to a small extent by CYP2C8, CYP2C9, and CYP2C19 (Chaumais *et al.*, 2015) it is well established that at a clinical relevant concentration, drug–drug interactions do not occur with coadministered drugs that are also substrates of CYP3A4 (Sidharta *et al.*, 2015).

In HepaRG cells, MAC and BOS caused deformation of BC and impairment of MLC2 phosphorylation that have previously been found to be characteristics of cholestatic drugs (Burbank *et al.*, 2016; Sharanek *et al.*, 2016) (Table 3). Contrary to the two other ERAs, AMB and SIT, which exhibit different chemical structures and are specific for ET_A receptors, MAC and BOS share a similar chemical structure (Supplementary Table 3) and reactivity with both ET_A and ET_B receptors. Macitentan and BOS structures differ only by addition of the replacement of the sulfonamide moiety by a smaller alkyl-sulfamide group in the former, resulting in an increased lipophilicity (Chaumais *et al.*, 2015).

Intrahepatic cholestasis is typically characterized by an inhibition of biliary efflux of BAs leading to their accumulation mostly in hepatocytes. As expected TCA and CDF efflux that reflects BSEP and MRP2 activity, respectively, was inhibited by both BOS and MAC, supporting a strong inhibition of canalicular efflux. These results as well as inhibition of NTCP agreed with several previous studies (Hartman *et al.*, 2010; Lepist *et al.*, 2014; Morgan *et al.*, 2013). However, some authors reported only weak inhibition if any, of BSEP with MAC (Treiber *et al.*, 2007) and MRP2 with BOS (Hartman *et al.*, 2010; Lepist *et al.*, 2014). These discrepancies likely reflect use of different experimental conditions. Such inhibitions of efflux and influx transporters are not specific of cholestatic drugs (Köck *et al.*, 2014; Pedersen *et al.*, 2013). As observed earlier (Hartman *et al.*, 2010; Kenna, 2014; Morgan *et al.*, 2013), SIT also inhibited TCA and CDF efflux activity in HepaRG cells. No BA accumulation was observed with any of the 4 ERAs in HepaRG cell cultures but on the contrary, total BAs content was decreased in cellular layers after 4 and 24 h treatment in a serum-free medium. A similar observation has been made by using sandwich-cultured human hepatocytes treated with these drugs (Lepist *et al.*, 2014). The decrease in total BAs content in cellular layers after treatment with BOS, MAC, and SIT could be related to MRP3 overexpression and consequently resulting in increased sinusoidal efflux. Multidrug resistance-associated protein 3 has been reported to be upregulated as a result of an adaptive mechanism to the inhibition of MRP2 and BSEP efflux (Donner and Keppler, 2001), including in HepaRG cells KO in BSEP (Qiu *et al.*, 2016). Noticeably, a 2.5-fold activation of TCA efflux after 2 h with a low concentration of SIT (ie, 10 μM), which has been described for troglitazone, entacapone, or diclofenac (Al-Attrache *et al.*, 2015.; Burbank *et al.*, 2016), was observed. An uncoupling effect between lipids and bile salt independent efflux at the MRP2 level has also been described in BOS-treated rats (Fouassier *et al.*, 2002). Whether a similar effect can occur in treated patients and in cultured human hepatocytes remains unknown.

Only BOS has been reported to cause some cases of cholestasis in clinic. Several explanations can be advanced to support the absence of reported clinical cases of cholestasis with MAC: (1) the approval of this drug received only in 2013 and consequently the limited number of patients treated to-date; (2) the different physico-chemical properties, pharmacokinetics, and metabolism profiles; (3) more likely conditions of administration to patients. Bosentan is dosed at 62.5 mg two times a day for 4 weeks before using a dose of 125 mg/day while MAC is active at 10 mg/day (Pulido *et al.*, 2013) and has a lower C_{max} in comparison with BOS; (4) its 15-fold increased receptor residence time ($t_{1/2}$) compared to BOS, that could explain at least partly its therapeutic effects at lower dosages (Gatfield *et al.*, 2012). Moreover, cholestatic features were obtained *in vitro* with BOS at lower concentrations (<100 μM) than with MAC. Noteworthy, an association of BOS and the direct ROCK inhibitor fasudil has been tested. Indeed, fasudil has been successfully used to reverse PAH findings in animal models (Liu *et al.*, 2011). However, no improvement of exercise capacity and pulmonary hemodynamics was evidenced after a 3-month treatment of PAH patients with fasudil (Fukumoto *et al.*, 2013). Moreover, our *in vitro* data showed that BOS-induced BC dilatation was strongly enhanced by coaddition of fasudil in HepaRG cells, suggesting that the combination of the two drugs could result in enhanced cholestatic effects (Supplementary Fig. 4).

In summary, our data demonstrate that the two ERAs, BOS, and MAC, share some typical cholestatic features which could be attributed to their similar chemical structures. However, these two drugs differ by several properties, in particular lower daily therapeutic dosages and C_{max}, and longer receptor residence time that could explain the absence of MAC toxicity presently reported in patients. In addition, our results support a relationship between SIT and BOS hepatotoxicity and the formation of CYP-mediated reactive metabolites. They also support the current recommendation to monitor liver enzymes at the initiation of MAC treatment and in the presence of clinical findings, and to discontinue therapy if patients develop sustained aminotransferase and bilirubin elevations (Monaco and Davila, 2016).

SUPPLEMENTARY DATA

Supplementary data are available at *Toxicological Sciences* online.

ACKNOWLEDGMENTS

We are grateful to Remy Le Guevel from the ImPACcell platform for imaging analysis.

FUNDING

This work was supported by the European Community through the Innovative Medicines Initiative Joint Undertaking MIP-DILI project [grant agreement number 115336], resources of which are composed of financial contribution from the European Union's Seventh Framework Programme [FP7/20072013] and EFPIA companies' in kind contribution. http://www.imi.europa.eu/. Matthew Burbank was financially supported ANRT (Association Nationale de la Recherche et de la Technologie) [n°2013/0112], and Ahmad Sharanek and Audrey Burban by the MIP-DILI project.

REFERENCES

Ahn, L. Y., Kim, S. E., Yi, S., Dingemanse, J., Lim, K. S., Jang, I.-J., and Yu, K.-S. (2014). Pharmacokinetic-pharmacodynamic relationships of macitentan, a new endothelin receptor antagonist, after multiple dosing in healthy Korean subjects. *Am. J. Cardiovasc. Drugs* **14**, 377–385.

Al-Attrache, H., Sharanek, A., Burban, A., Burbank, M., Gicquel, T., Abdel-Razzak, Z., Guguen-Guillouzo, C., Morel, I., and Guillouzo, A. (2015). Differential sensitivity of metabolically competent and non-competent HepaRG cells to apoptosis induced by diclofenac combined or not with TNF-α. *Toxicol. Lett.* **58**, 71–85.

Aninat, C., Piton, A., Glaise, D., Le Charpentier, T., Langouët, S., Morel, F., Guguen-Guillouzo, C., and Guillouzo, A. (2006). Expression of cytochromes P450, conjugating enzymes and nuclear receptors in human hepatoma HepaRG cells. *Drug Metab. Dispos.* **34**, 75–83.

Anthérieu, S., Bachour-El Azzi, P., Dumont, J., Abdel-Razzak, Z., Guguen-Guillouzo, C., Fromenty, B., Robin, M.-A., and Guillouzo, A. (2013). Oxidative stress plays a major role in chlorpromazine-induced cholestasis in human HepaRG cells. *Hepatology* **57**, 1518–1529.

Bachour-El Azzi, P., Sharanek, A., Burban, A., Li, R., Guével, R. L., Abdel-Razzak, Z., Stieger, B., Guguen-Guillouzo, C., and Guillouzo, A. (2015). Comparative localization and functional activity of the main hepatobiliary transporters in HepaRG cells and primary human hepatocytes. *Toxicol. Sci.* **145**, 157–168.

Barst, R. J. (2007). A review of pulmonary arterial hypertension: Role of ambrisentan. *Vasc. Health Risk Manag.* **3**, 11–22.

Ben-Yehuda, O., Pizzuti, D., Brown, A., Littman, M., Gillies, H., Henig, N., and Peschel, T. (2012). Long-term hepatic safety of ambrisentan in patients with pulmonary arterial hypertension. *J. Am. Coll. Cardiol.* **60**, 80–81.

Bolli, M. H., Boss, C., Binkert, C., Buchmann, S., Bur, D., Hess, P., Iglarz, M., Meyer, S., Rein, J., Rey, M., *et al.* (2012). The discovery of N-[5-(4-bromophenyl)-6-[2-[(5-bromo-2-pyrimidinyl)oxy]ethoxy]-4-pyrimidinyl]-N'-propylsulfamide (Macitentan), an orally active, potent dual endothelin receptor antagonist. *J. Med. Chem.* **55**, 7849–7861.

Bruderer, S., Hopfgartner, G., Seiberling, M., Wank, J., Sidharta, P. N., Treiber, A., and Dingemanse, J. (2012). Absorption, distribution, metabolism, and excretion of macitentan, a dual endothelin receptor antagonist, in humans. *Xenobiotica* **42**, 901–910.

Burbank, M. G., Burban, A., Sharanek, A., Weaver, R. J., Guguen-Guillouzo, C., and Guillouzo, A. (2016). Early alterations of bile canaliculi dynamics and the ROCK/MLCK pathway are characteristics of drug-induced intrahepatic cholestasis. *Drug Metab. Dispos.* **44**, 1780–1793.

Cerec, V., Glaise, D., Garnier, D., Morosan, S., Turlin, B., Drenou, B., Gripon, P., Kremsdorf, D., Guguen-Guillouzo, C., and Corlu, A. (2007). Transdifferentiation of hepatocyte-like cells from the human hepatoma HepaRG cell line through bipotent progenitor. *Hepatology* **45**, 957–967.

Chaumais, M.-C., Guignabert, C., Savale, L., Jaïs, X., Boucly, A., Montani, D., Simonneau, G., Humbert, M., and Sitbon, O. (2015). Clinical pharmacology of endothelin receptor antagonists used in the treatment of pulmonary arterial hypertension. *Am. J. Cardiovasc. Drugs* **15**, 13–26.

Croxtall, J. D., and Keam, S. J. (2008). Ambrisentan. *Drugs* **68**, 2195–2204.

D'Alonzo, G. E., Barst, R. J., Ayres, S. M., Bergofsky, E. H., Brundage, B. H., Detre, K. M., Fishman, A. P., Goldring, R. M., Groves, B. M., and Kernis, J. T. (1991). Survival in patients with primary pulmonary hypertension. Results from a national prospective registry. *Ann. Intern. Med.* **115**, 343–349.

Davenport, A. P., and Battistini, B. (2002). Classification of endothelin receptors and antagonists in clinical development. *Clin. Sci.* **103(Suppl. 48)**, 1S–3S.

Dawson, S., Stahl, S., Paul, N., Barber, J., and Kenna, J. G. (2012). In vitro inhibition of the bile salt export pump correlates with risk of cholestatic drug-induced liver injury in humans. *Drug Metab. Dispos.* **40**, 130–138.

de Abajo, F. J., Montero, D., Madurga, M., and García Rodríguez, L. A. (2004). Acute and clinically relevant drug-induced liver injury: A population based case-control study. *Br. J. Clin. Pharmacol.* **58**, 71–80.

Dhaun, N., Melville, V., Kramer, W., Stavros, F., Coyne, T., Swan, S., Goddard, J., and Webb, D. J. (2007). The pharmacokinetic profile of sitaxsentan, a selective endothelin receptor antagonist, in varying degrees of renal impairment. *Br. J. Clin. Pharmacol.* **64**, 733–737.

Dhillon, S., and Keating, G. M. (2009). Bosentan: A review of its use in the management of mildly symptomatic pulmonary arterial hypertension. *Am. J. Cardiovasc. Drugs* **9**, 331–350.

Donner, M. G., and Keppler, D. (2001). Up-regulation of basolateral multidrug resistance protein 3 (Mrp3) in cholestatic rat liver. *Hepatology* **34**, 351–359.

Dupuis, J., and Hoeper, M. M. (2008). Endothelin receptor antagonists in pulmonary arterial hypertension. *Eur. Respir. J.* **31**, 407–415.

Erve, J. C. L., Gauby, S., Maynard, J. W., Svensson, M. A., Tonn, G., and Quinn, K. P. (2013). Bioactivation of sitaxentan in liver microsomes, hepatocytes, and expressed human P450s with characterization of the glutathione conjugate by liquid chromatography tandem mass spectrometry. *Chem. Res. Toxicol.* **26**, 926–936.

Fattinger, K., Funk, C., Pantze, M., Weber, C., Reichen, J., Stieger, B., and Meier, P. J. (2001). The endothelin antagonist bosentan inhibits the canalicular bile salt export pump: A potential mechanism for hepatic adverse reactions. *Clin. Pharmacol. Ther.* **69**, 223–231.

Fouassier, L., Kinnman, N., Lefèvre, G., Lasnier, E., Rey, C., Poupon, R., Elferink, R. P. J. O., and Housset, C. (2002). Contribution of mrp2 in alterations of canalicular bile formation by the endothelin antagonist bosentan. *J. Hepatol.* **37**, 184–191.

Fukumoto, Y., Yamada, N., Matsubara, H., Mizoguchi, M., Uchino, K., Yao, A., Kihara, Y., Kawano, M., Watanabe, H., Takeda, Y., *et al.* (2013). Double-blind, placebo-controlled

clinical trial with a rho-kinase inhibitor in pulmonary arterial hypertension. *Circ. J.* **77**, 2619–2625.

Galiè, N., Hoeper, M. M., Gibbs, J. S. R., and Simonneau, G. (2011). Liver toxicity of sitaxentan in pulmonary arterial hypertension. *Eur. Respir. J.* **37**, 475–476.

Gatfield, J., Grandjean, C. M., Sasse, T., Clozel, M., and Nayler, O. (2012). Slow receptor dissociation kinetics differentiate macitentan from other endothelin receptor antagonists in pulmonary arterial smooth muscle cells. *PLOS One* **7**, e47662.

Ghofrani, H. A., Distler, O., Gerhardt, F., Gorenflo, M., Grünig, E., Haefeli, W. E., Held, M., Hoeper, M. M., Kähler, C. M., Kaemmerer, H., *et al.* (2011). Treatment of pulmonary arterial hypertension (PAH): Updated recommendations of the cologne consensus conference 2011. *Int. J. Cardiol.* **154(Suppl. 1)**, S20–S33.

Hartman, J. C., Brouwer, K., Mandagere, A., Melvin, L., and Gorczynski, R. (2010). Evaluation of the endothelin receptor antagonists ambrisentan, darusentan, bosentan, and sitaxsentan as substrates and inhibitors of hepatobiliary transporters in sandwich-cultured human hepatocytes. *Can. J. Physiol. Pharmacol.* **88**, 682–691.

Humbert, M., Sitbon, O., and Simonneau, G. (2004). Treatment of pulmonary arterial hypertension. *N. Engl. J. Med.* **351**, 1425–1436.

Kenna, J. G. (2014). Current concepts in drug-induced bile salt export pump (BSEP) interference. *Curr. Protoc. Toxicol.* **61**, 23.7.1–15.

Köck, K., Ferslew, B. C., Netterberg, I., Yang, K., Urban, T. J., Swaan, P. W., Stewart, P. W., and Brouwer, K. L. R. (2014). Risk factors for development of cholestatic drug-induced liver injury: Inhibition of hepatic basolateral bile acid transporters multidrug resistance-associated proteins 3 and 4. *Drug Metab. Dispos.* **42**, 665–674.

Lavelle, A., Sugrue, R., Lawler, G., Mulligan, N., Kelleher, B., Murphy, D. M., and Gaine, S. P. (2009). Sitaxentan-induced hepatic failure in two patients with pulmonary arterial hypertension. *Eur. Respir. J.* **34**, 770–771.

Lepist, E.-I., Gillies, H., Smith, W., Hao, J., Hubert, C., Claire, I. I. I. R. L. S., Brouwer, K. R., and Ray, A. S. (2014). Evaluation of the endothelin receptor antagonists ambrisentan, bosentan, macitentan, and sitaxsentan as hepatobiliary transporter inhibitors and substrates in sandwich-cultured human hepatocytes. *PLoS One* **9**, e87548.

Lin, Y.-L., Wu, Y.-C., Gau, C.-S., and Lin, M.-S. (2012). Value of preapproval safety data in predicting postapproval hepatic safety and assessing the legitimacy of class warning. *Ther. Adv. Drug Saf.* **3**, 13–24.

Liu, A.-J., Ling, F., Wang, D., Wang, Q., Lü, X.-D., and Liu, Y-L. (2011). Fasudil inhibits platelet-derived growth factor-induced human pulmonary artery smooth muscle cell proliferation by up-regulation of p27kip^{1} via the ERK signal pathway. *Chin. Med. J.* **124**, 3098–3104.

Mano, Y., Usui, T., and Kamimura, H. (2007). Effects of bosentan, an endothelin receptor antagonist, on bile salt export pump and multidrug resistance-associated protein 2. *Biopharm. Drug Dispos.* **28**, 13–18.

Matsunaga, N., Kaneko, N., Staub, A. Y., Nakanishi, T., Nunoya, K., Imawaka, H., and Tamai, I. (2016). Analysis of the metabolic pathway of bosentan and of the cytotoxicity of bosentan metabolites based on a quantitative modeling of metabolism and transport in sandwich-cultured human hepatocytes. *Drug Metab. Dispos.* **44**, 16–27.

McLaughlin, V. V., Davis, M., and Cornwell, W. (2011). Pulmonary arterial hypertension. *Curr. Probl. Cardiol.* **36**, 461–517.

Miao, L., Dai, Y., and Zhang, J. (2002). Mechanism of RhoA/Rho kinase activation in endothelin-1-induced contraction in rabbit basilar artery. *Am. J. Physiol. Heart Circ. Physiol.* **283**, H983–H989.

Monaco, T. J., and Davila, C. D. (2016). Safety, efficacy, and clinical utility of macitentan in the treatment of pulmonary arterial hypertension. *Drug Des. Dev. Ther.* **10**, 1675–1682.

Morgan, R. E., van Staden, C. J., Chen, Y., Kalyanaraman, N., Kalanzi, J., Dunn, R. T., Afshari, C. A., and Hamadeh, H. K. (2013). A multifactorial approach to hepatobiliary transporter assessment enables improved therapeutic compound development. *Toxicol. Sci.* **136**, 216–241.

Owen, K., Cross, D. M., Derzi, M., Horsley, E., and Stavros, F. L. (2012). An overview of the preclinical toxicity and potential carcinogenicity of sitaxentan (Thelin®), a potent endothelin receptor antagonist developed for pulmonary arterial hypertension. *Regul. Toxicol. Pharmacol.* **64**, 95–103.

Pauli-Magnus, C., and Meier, P. J. (2006). Hepatobiliary transporters and drug-induced cholestasis. *Hepatology* **44**, 778–787.

Peacock, A. J., Murphy, N. F., McMurray, J. J. V., Caballero, L., and Stewart, S. (2007). An epidemiological study of pulmonary arterial hypertension. *Eur. Respir. J.* **30**, 104–109.

Pedersen, J. M., Matsson, P., Bergström, C. A. S., Hoogstraate, J., Norén, A., LeCluyse, E. L., and Artursson, P. (2013). Early identification of clinically relevant drug interactions with the human bile salt export pump (BSEP/ABCB11). *Toxicol. Sci.* **136**, 328–343.

Pernelle, K., Le Guevel, R., Glaise, D., Stasio, C. G.-D., Le Charpentier, T., Bouaita, B., Corlu, A., and Guguen-Guillouzo, C. (2011). Automated detection of hepatotoxic compounds in human hepatocytes using HepaRG cells and image-based analysis of mitochondrial dysfunction with JC-1 dye. *Toxicol. Appl. Pharmacol.* **254**, 256–266.

Pulido, T., Adzerikho, I., Channick, R. N., Delcroix, M., Galiè, N., Ghofrani, H.-A., Jansa, P., Jing, Z.-C., Le Brun, F.-O., Mehta, S., *et al.* (2013). Macitentan and morbidity and mortality in pulmonary arterial hypertension. *N. Engl. J. Med.* **369**, 809–818.

Qiu, X., Zhang, Y., Liu, T., Shen, H., Xiao, Y., Bourner, M. J., Pratt, J. R., Thompson, D. C., Marathe, P., Humphreys, W. G., *et al.* (2016). Disruption of BSEP Function in HepaRG cells alters bile acid disposition and is a susceptive factor to drug-induced cholestatic injury. *Mol. Pharm.* **13**, 1206–1216.

Raja, S. G. (2010). Macitentan, a tissue-targeting endothelin receptor antagonist for the potential oral treatment of pulmonary arterial hypertension and idiopathic pulmonary fibrosis. *Curr. Opin. Investig. Drugs* **11**, 1066–1073.

Sharanek, A., Bachour-El Azzi, P., Al-Attrache, H., Savary, C. C., Humbert, L., Rainteau, D., Guguen-Guillouzo, C., and Guillouzo, A. (2014). Different dose-dependent mechanisms are involved in early cyclosporine a-induced cholestatic effects in hepaRG cells. *Toxicol. Sci.* **141**, 244–253.

Sharanek, A., Burban, A., Humbert, L., Bachour-El Azzi, P., Felix-Gomes, N., Rainteau, D., and Guillouzo, A. (2015). Cellular Accumulation and Toxic Effects of Bile Acids in Cyclosporine A-Treated HepaRG Hepatocytes. *Toxicol Sci.* **147**(2), 573–587.

Sharanek, A., Burban, A., Burbank, M., Le Guevel, R., Li, R., Guillouzo, A., and Guguen-Guillouzo, C. (2016). Rho-kinase/myosin light chain kinase pathway plays a key role in the impairment of bile canaliculi dynamics induced by cholestatic drugs. *Sci. Rep.* **6**, 24709.

Sidharta, P. N., Krähenbühl, S., and Dingemanse, J. (2015). Pharmacokinetic and pharmacodynamic evaluation of macitentan, a novel endothelin receptor antagonist for the

treatment of pulmonary arterial hypertension. *Expert Opin. Drug Metab. Toxicol.* **11**, 437–449.

Sidharta, P. N., van Giersbergen, P. L. M., Halabi, A., and Dingemanse, J. (2011). Macitentan: Entry-into-humans study with a new endothelin receptor antagonist. *Eur. J. Clin. Pharmacol.* **67**, 977–984.

Simonneau, G., Galiè, N., Jansa, P., Meyer, G. M. B., Al-Hiti, H., Kusic-Pajic, A., Lemarié, J.-C., Hoeper, M. M., and Rubin, L. J. (2014). Long-term results from the EARLY study of bosentan in WHO functional class II pulmonary arterial hypertension patients. *Int. J. Cardiol.* **172**, 332–339.

Sood, N. (2014). Macitentan for the treatment of pulmonary arterial hypertension. *Expert Opin. Pharmacother.* **15**, 2733–2739.

Stavros, F., Kramer, W. G., and Wilkins, M. R. (2010). The effects of sitaxentan on sildenafil pharmacokinetics and pharmacodynamics in healthy subjects. *Br. J. Clin. Pharmacol.* **69**, 23–26.

Takatsuki, S., Rosenzweig, E. B., Zuckerman, W., Brady, D., Calderbank, M., and Ivy, D. D. (2013). Clinical safety, pharmacokinetics, and efficacy of ambrisentan therapy in children with pulmonary arterial hypertension. *Pediatr. Pulmonol.* **48**, 27–34.

Treiber, A., Schneiter, R., Hausler, S., and Stieger, B. (2007). Bosentan is a substrate of human OATP1B1 and OATP1B3: Inhibition of hepatic uptake as the common mechanism of its interactions with cyclosporin A, rifampicin, and sildenafil. *Drug Metab. Dispos.* **35**, 1400–1407.

Velayati, A., Valerio, M. G., Shen, M., Tariq, S., Lanier, G. M., and Aronow, W. S. (2016). Update on pulmonary arterial hypertension pharmacotherapy. *Postgrad. Med.* **128**, 460–473.

Weiss, J., Theile, D., Spalwisz, A., Burhenne, J., Riedel, K.-D., and Haefeli, W. E. (2013). Influence of sildenafil and tadalafil on the enzyme- and transporter-inducing effects of bosentan and ambrisentan in LS180 cells. *Biochem. Pharmacol.* **85**, 265–273.